VOL. 17, NO. 9, MAY 2022 ISSN 1819-6608
ARPN Journal of Engineering and Applied Sciences

www.arpnjournals.com

ANALYSIS OF THE STRESS-DEFORMED STATE OF ELEMENTS OF TRANSVERSE LOAD-BEARING SECTIONS OF BUSES USING METHODS OF FINITE-ELEMENT MODELING APPROACH

Ovchinnikov N. A.
Don State Technical University, Rostov Region, Shakhty, Ul Shevchenko, Russia
E-Mail: NikolaOv@yandex.ru

ABSTRACT

The article presents the results of a numerical study examining load-bearing capacity for cross sectional elements of a bus (in particular side window struts\posts). The author offers the implementation of the finite-elemental method analysis of the stress-strain state, using the ANSYS application package for a bus window post when bent where chemical corrosion of the material was taken into consideration. The numerical study of the load-bearing was carried out for a console fixed rack during bending in the plane which is perpendicular to the axis of the bus, taking into account the geometric and physical nonlinearity of the material in combination with a decrease in the thickness of the structure due to the corrosion of the metal, and for a truncated post with force applied at an angle to the loading site under the same conditions. A series of computational experiments was provided for an integral rack with localised corrosion. The conditions and boundaries for the subsequent finite-element modeling of cross sectional elements of a bus were considered constant for the purpose of this article.

Keywords: bus, body, body pillar, passive safety, strength, geometric nonlinearity, physical nonlinearity, body deformation, breaking load, safe service life, residual life.

INTRODUCTION

When conducting structural analysis of medium and large class buses, it can be concluded that their safety under rollover conditions according to UNECE Regulations No. 66 [1] can be determined by the total resistance to fracture of their individual constituent sections: front end, rear end, middle sections, which may change over time [2]. In the case of a bus overturning according to the procedure outlined in the Rules, the entire impact energy [3, 4] leading to symmetric destruction is absorbed to a greater extent by the sections of the body and its elements. Each such section is a closed rectangular frame, which includes a roof arch, two inter-window struts of the sidewalls with adjacent brackets (reinforcements), and a beam at the base [5].

The longitudinal elements of the roof (stringers), the cant and waist rails, as well as the sidewall panels themselves, in the event of lateral overturning, provide only the connection of the transverse load-bearing sections with each other and practically do not take on significant lateral loads. Therefore, when assessing the safety of the body structure, the decisive role is played by the strength of the sections and, in particular, by the struts of the window frames.

The main goal, in this case, is to conduct a numerical study of the bearing capacity of the side interwindow struts of the bus body during bending, taking into account the geometric and physical nonlinearity of the material in combination with a decrease in the thickness of the structure due to metal corrosion.

The assessment involves the analysis of the results of computer modeling of detailed finite element models of body structures, accounting for all their features [6, 7].

MATERIALS AND METHODS

The calculation of a detailed finite element model will be performed taking into account the physical and geometric nonlinearity, which makes it possible to obtain all the necessary characteristics of the structure (the nature of body deformability, the magnitude of the breaking load, energy consumption).

The implementation is hereinafter offered of the finite element analysis of the stress-strain state of a strut during bending, taking into account the effect of chemical corrosion of the material on the stiffness and strength characteristics of the strut, using the capabilities of the ANSYS application software package [8].

Figure-1 shows a solid model of a box-shaped window post of a LiAZ-5256 bus. The post is a thin-walled structural element. It is made by cold stamping of separate fragments from a steel sheet 2 mm thick, which are then welded together. Observations have shown that during operation, window racks of buses are subject to uniform corrosive wear along the entire inner surface, as well as intense local corrosion in the lower and upper parts of these structures [9-17].

Both, left and right, sides of a LiAZ-5256 body have six inter-window racks. As a supporting structural element, this part plays an important role in ensuring the rigidity of the bus body, especially in the event of an emergency situation specifically overturning of the vehicle subject to lateral forces at an angle of more than 90°.

To analyze the effect of chemical corrosion on the stiffness and strength characteristics of the rack, three sets of calculations were performed.

In the first set of calculations, a numerical study was carried out focusing on the dependence between the load-bearing capacity of a cantilever-mounted strut during bending in the plane perpendicular to the axis of the bus

with the geometric and physical nonlinearity of the material and a decrease in the thickness of the structure due to metal corrosion. An artificially truncated strut was used as an object of research (Fig. 2). The force is applied to a round platform with the diameter of 50 mm and thickness of 10 mm, located in the upper part of the post at a distance of 830 mm from the base. Taking into account the axial symmetry of the geometry and loading scheme, in order to save computational resources, we will consider only half the rack (Fig. 3).

The finite element mesh built on the basis of the SHELL43 laminar plate is shown in Fig. 4. The figure shows surfaces of the rack at the base and where the load is applied. As a result of discretization of only half the rack into finite elements, the number of nodes in the design scheme was 727; the number of triangular plate elements is 1305.

The global Cartesian coordinate system is chosen for the system with the origin located at the lowest point of the strut. In this case, the X axis is directed horizontally; Y-axis - vertically along the axis of symmetry; Z-axis - perpendicular to the front surfaces. In order to exclude displacements of the finite element model "as a rigid whole", the base of the rack is rigidly fixed to the supporting surface. On the nodes located in the plane of symmetry Y0Z, we impose constraints that prohibit linear displacements in the direction of the X axis and angular displacements relative to the Y and Z axes.

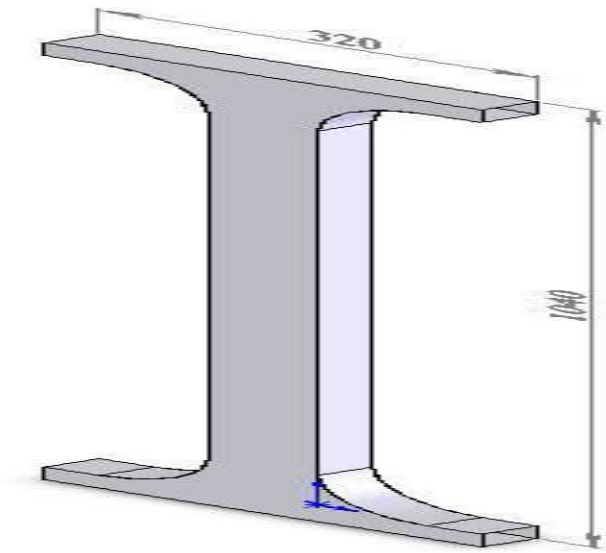

Figure-1. Post model for LiAZ-5256.

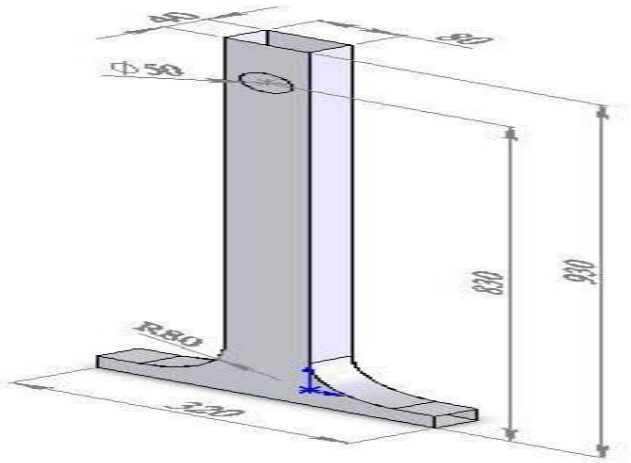

Figure-2. Model for a truncated post.

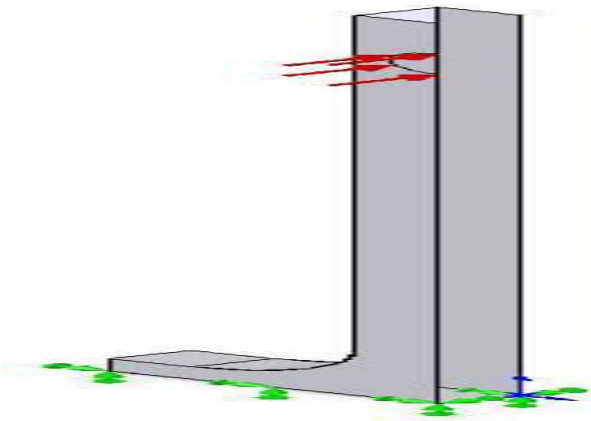

Figure-3. Model of a half artificially truncated rack.

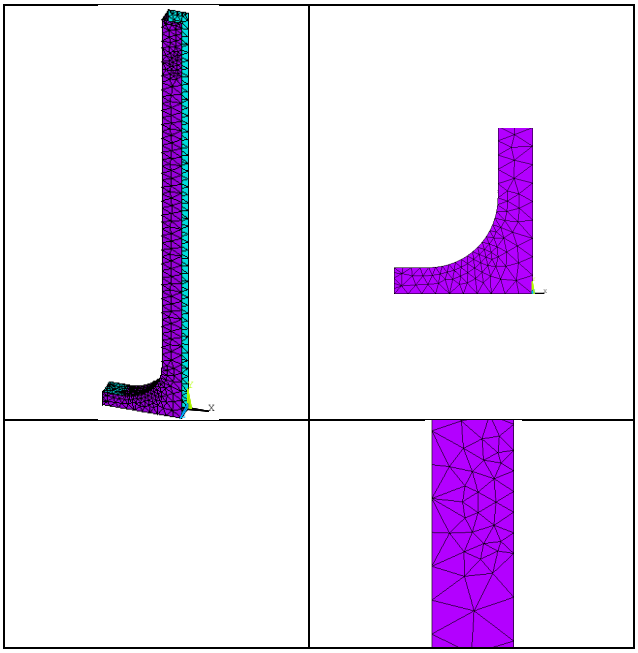

Figure-4. A finite element grid constructed on the basis of a plate finite element of the SHELL43 type.

Mechanical constants of the material (steel): modulus of elasticity E = 2.05 · 105 MPa; Poisson's ratio ν= 0.28; yield point σ_T= 2.83 · 102 MPa. To take into account the physical nonlinearity of the material, we use the model of an ideally plastic body.

The results of finite element modeling of the strut bending taking into account geometric and physical nonlinearity are shown in Figures 5 and 6. Figure-5 shows the dependence of the maximum deflection of the post f on the load P and the degree of corrosive wear of the material. As mentioned above, as a first approximation, corrosion wear is taken into account by uniformly reducing the thickness of the sheet over the entire surface of the rack, with the exception of the round area to which the load is applied and the fastening surface. Line numbers 1, 2, 3, 4 on the P vs. f graph correspond to sheet thicknesses 2.0 mm (intact post), 1.9 mm (2 years of operation), 1.8 mm (2 years of operation), 1.6 mm (6 years operation).

Comparing the curves in Figure-5, we come to quite a natural conclusion that a uniform decrease in thickness over the entire surface of the material leads to a corresponding decrease in the maximum load at which the strut exhausts its load-bearing capacity. It was found that with a further increase in the load, the iterative process is interrupted, the so-called "vertical break" on the graph.

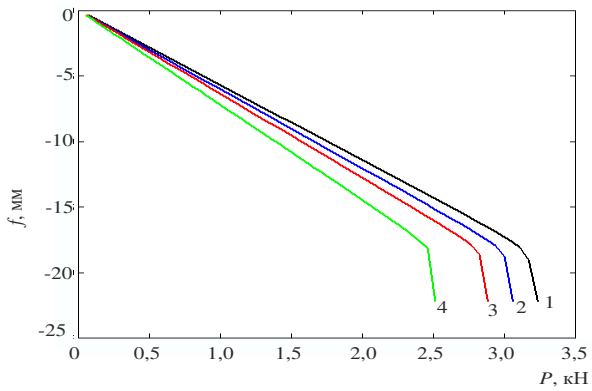

Figure-5. Dependence of maximum deflection on the load applied with varying degrees of corrosion.

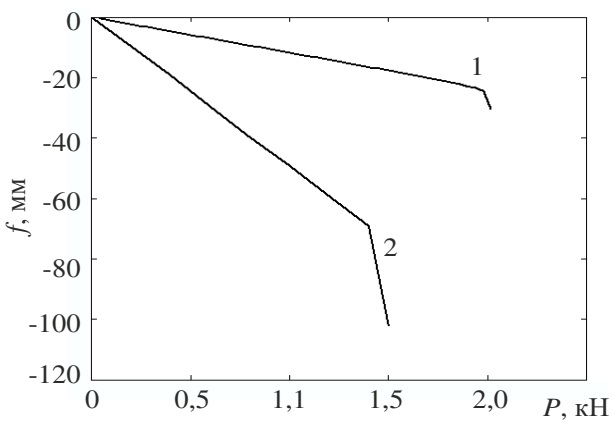

Figure-6. Comparison between finite element model data (line 1) and experimental data (line 2).

Figure-6 shows the P vs. f graphs obtained using numerical (line 1) and laboratory (line 2) experiments. The numerical solution describes the curve of equilibrium states, corresponding to a rack thickness of 1.6 mm (6 years of operation). The experimental curve was constructed based on the results of full-scale bending tests of the truncated body post of the MAN SL200 bus [10], which had been in operation for 28 years and had a mileage of 920 thousand km. Comparing the curves of the equilibrium states of the real and virtual struts, we find a qualitative coincidence of the results. The racks are of comparable dimensions. At the same time, the loss of the load-bearing capacity of the real post occurs at a significantly higher deflection value (about 70 mm), while the virtual post loses its bearing capacity at a deflection value of 23 mm. The explanation for this phenomenon, apparently, lies in the way the boundary conditions are set in the numerical simulation in the form of a rigid termination at the base of the strut. In practice, the nature of the connection of the lower base of the strut with the bus frame provides for some flexibility in the console part, which explains its much greater movement.

Pictures of stress intensity distribution, σ_i, in the form of contour fields for an intact strut are shown in Figure-7. Modeling of the load P was carried out with the following steps: 0.648 kN; 1.3 kN; 1.94 kN; 2.59 kN; 3.24 kN. The visualization is made for the lower most loaded part of the strut. On the left, a fragment of the base of the strut is shown from the loading side, on the right is a fragment of the base from the rear side of the strut for two load options: initial (0.648 kN) and final (3.24 kN).

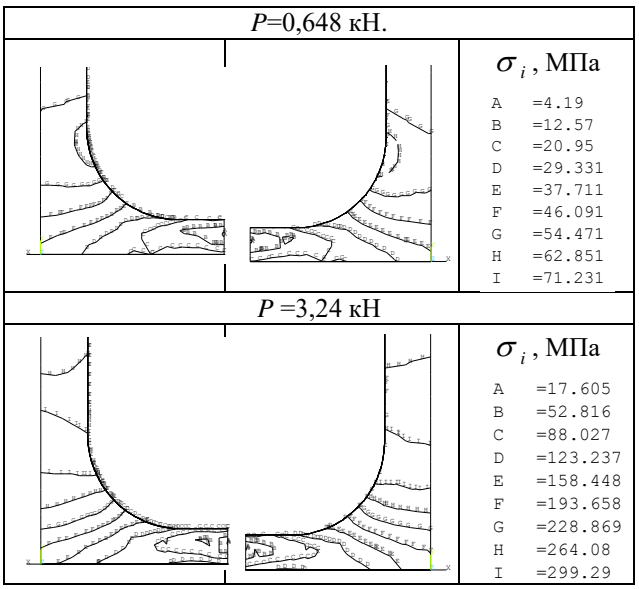

Figure-7. Stress intensity distribution (contour fields) for an intact strut.

In the linear section of deformation, the picture of the stress state practically does not change, i.e., a similarity of isolines of the stress field is observed. When a plastic response of the material to an increase in load appears, a sharp redistribution of stresses in the

concentration zone occurs. As you can see, when the value of the force P = 3.24 kN is reached, a plastic hinge is formed (isoline I), and the post loses its load-bearing capacity.

In the second set of calculations, a series of computational experiments was carried out for a non-truncated strut loaded with a concentrated force at an angle to the loading area. In this case, the rack will experience a complex bend. This type of loading is most typical in an emergency situation associated with a bus overturning whilst moving at low speed. Figures 8 and 9 show, respectively, the design scheme of the rack and the finite element mesh. The total number of SHELL43 elements was 4304; the total number of nodes was 2194. The decomposition of a concentrated force applied at an angle to an area with a diameter of 50 mm at a distance of 1000 mm from the base is carried out according to the following formulas:

$$P_x = P\cos\alpha\,;\;\; P_y = P\cos\beta\,;\;\; P_z = P\cos\gamma\,,$$

where α, β and γ are the angles between the vector P and the X, Y, Z axes.

The angles are set to: α= 77°; β= 75°. Here the value of the angle is determined by the formula:

$$\gamma = \sqrt{1-(\cos^2\alpha + \cos^2\beta)}\,.$$

After substituting the corresponding values, we get γ= 20.05°.

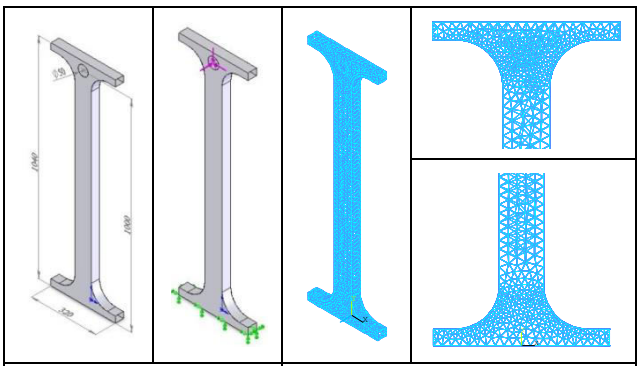

Figure-8. Design diagram of the strut. **Figure-9.** Finite element mesh.

The results of numerical calculations are shown in Figure-10. f_z is the displacement of the force along the Z axis.

The same as for the truncated post, the line numbers 1, 2, 3, 4 correspond to sheet thicknesses of 2.0 mm (intact post), 1.9 mm (2 years of operation), 1.8 mm (2 years of operation) and 1.6 mm (6 years of operation).

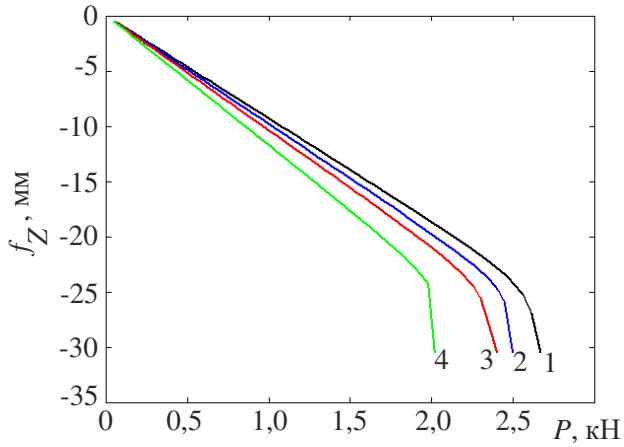

Figure-10. Results of finite element modeling of a non-truncated strut showing the dependence of the maximum deflection of the strut f on the load P and the degree of corrosive wear of the material.

Comparing the corresponding curves in Figures 5 and 10, it is established that the patterns of the loss of the load-bearing capacity of the non-truncated and truncated struts are similar. A distinctive feature is that for a non-truncated strut, "vertical stall" on the graph is observed at lower load values. But this is due to the greater value of the "lever" for the force applied in the non-truncated strut scheme.

Figure-11 shows the calculation results for the lower part of the intact strut in the form of isolines of the stress intensity distribution, σ_i, at different load levels, P, equal to: 0.534 kN; 1.068 kN; 1.60 kN; 2.14 kN; 2.56 kN; 2.61 kN; 2.67 kN. On the left, a fragment of the base of the strut from the loading side is shown, on the right is a fragment of the base from the rear side of the strut for two load options: initial (0.534 kN) and final (2.67 kN).

Graphical data for a complex bending of a cantilevered strut is presented in Figure-11, it can be concluded that the method of applying the load significantly affects the type of stress state in the lower most loaded part of the post. In particular, we establish that the plastic zone where the load is applied extends over a much smaller area than on the opposite surface of the post. Hence, it is possible to propose, as a practical recommendation for designers, a method of strengthening the lower parts of the window frames from the inside of the cabin.

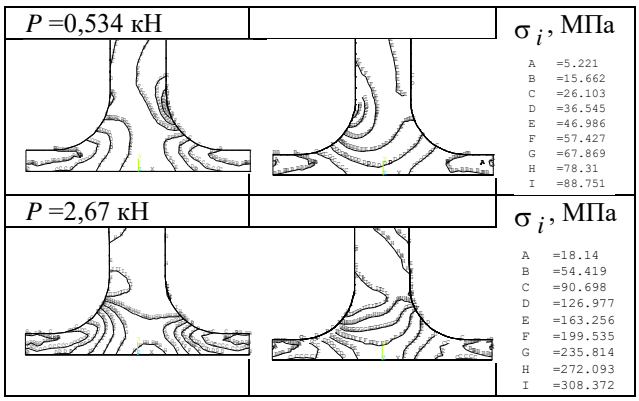

Figure-11. Stress intensity distribution in the form of contour fields for an intact bus body strut.

In the third and final set of calculations, a non-truncated strut 1.8 mm thick (4 years of operation) with localised corrosion damage in the lower part from the front side was simulated. Areas of local damage are shown in dark color in Figure-12, which is a finite element sampling diagram of the bottom of the strut.

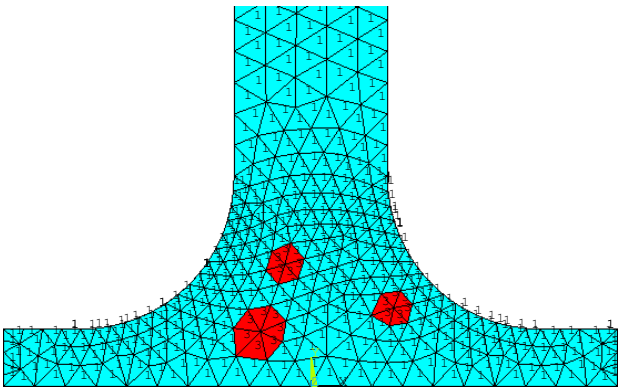

Figure-12. Zones of local damage on the finite element discretization diagram of the lower part of the strut.

During calculations, it is assumed that in the indicated local zones the modulus of elasticity of the material is two orders of magnitude less than the modulus of elasticity of the base material of the strut. Poisson's ratio in these zones is taken to be zero. A force is applied to a round platform with a diameter of 50 mm in the upper part of the strut at an angle, as in the previous version.

Figure-13 shows the deformation curves for a strut without corrosion (line 1) and a strut with localised damage (line 2).

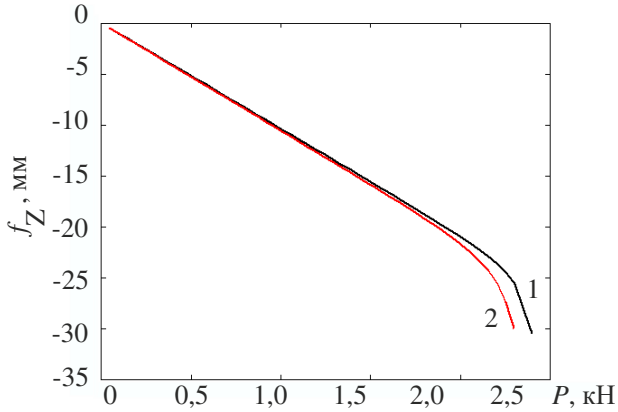

Figure-13. FEM results for a strut without corrosive damage and a strut with localised corrosion.

As it can be observed, the presence of localised corrosion leads to a decrease in the overall rigidity of the strut, which leads to a decrease in the load-bearing capacity of the structure. With visual examination of the control group of buses, it was found that damage to window struts due to corrosion increases with every year, especially during the autumn-winter period of operation. It should be noted that in the conditions of long-term operation of the bus fleet, corrosion is observed on almost all buses, both imported and domestically produced. Moreover, this type of body wear cannot be repaired, but requires mandatory write-off of the bus with subsequent compulsory disposal in the presence of an expert group.

Figure-14 shows the results of FEM modelling as isolines of the plastic deformations intensity, ε_i, and the intensity of stresses, σ_i, for various levels of cantilever loading of the strut with a concentrated force P with values: 1.61 kN; 1.84 kN; 2.07 kN; 2.3 kN. Visualisation of the data is presented for the area of the rack affected by corrosion for two load options: initial (1.61 kN) and final (2.3 kN). The contours of areas affected by corrosion are highlighted by lines.

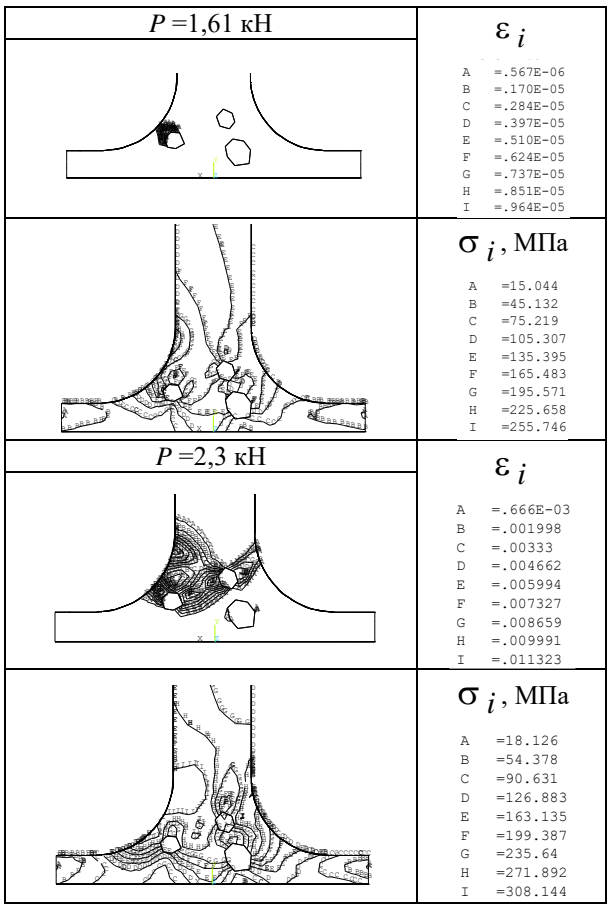

Figure-14. Contour fields for the area of the strut affected by corrosion.

The presence of local areas with an artificially reduced modulus of elasticity introduces significant inhomogeneity in the stress-strain state of the most loaded part of the strut. At the same time, a sharp gradient of the stress intensity field between these areas is observed, which in practice can lead to the appearance of microcracks at the edges of these zones.

CONCLUSIONS

Analysing the conducted research, one can come to the following conclusions:

- a uniform decrease in the thickness of the struts over the entire surface, due to the effect of corrosion, leads to a corresponding decrease in the maximum load value at which the strut exhausts its load-bearing capacity;
- visual comparison of the curves for equilibrium states obtained with the help of numerical and field experiments on the strut at bending, a qualitative correlation between the results is found;
- the model of a complex bending of a cantilevered strut indicates that the method of applying the load significantly affects the type of stress state in the lower most loaded part of the strut. Hence, it is possible to propose, as a practical recommendation for designers, to envisage a method of strengthening the lower parts of the window struts from the inside of the cabin;
- comparing the curves of equilibrium states for the non-truncated and truncated struts, we establish that the patterns of the loss of bearing capacity are similar;
- the presence of localised corrosion leads to a decrease in the overall stiffness of the strut, which leads to a decrease in the bearing capacity of the structure as a whole. Visual examination of the control group of buses, it was found that the surface of damage to window struts by corrosion increases with years, especially in the autumn-winter period of operation;
- the presence of local areas with an artificially reduced modulus of elasticity (modeling of corrosion foci) introduces significant inhomogeneity in the stress-strain state of the most loaded part of the strut.

REFERENCES

[1] GOST P 41.66-00 (UNECE Regulations No. 66). 2000. Uniform instructions concerning the approval of large-size passenger vehicles in a durability relationship of the upper structure. Brought on 26 May 1999, No. 184. Moscow: PPC Publishing House of standards. pp. 19.

[2] Kalmikov B. Yu., Ovchinnikov N. A., Kalmikova O. M., Jigulskii V. I. and Yurshin Yu. G. 2015. Proposals for determining the impact energy at bus rollover for conditions of UNECE №66. ARPN Journal of Engineering and Applied Sciences. 10(8): 3793-3797.

[3] Kalmikov B. Yu., Ovchinnikov N. A., Kalmikova O. M., Guguyev I. K. and Kushnariva I. V. 2015. Application of the method of distribution of the total energy of impact on the bearing elements of the body of the bus when calculating the failure loads. ARPN Journal of Engineering and Applied Sciences. 10(10): 4366-4371.

[4] Kalmikov B. Y., Visotski I. Y., Ovchinnikov N. A., Petriashvili I. M. and Kalmikova Y. B. 2015. The use of additional devices for reducing the deformation of the bus body when tipping. ARPN Journal of Engineering and Applied Sciences. 10(12): 5150-5156.

[5] Ovchinnikov N. A., Kalmikov B. Y., Stradanchenko S. G., Kozyreva E. A., Chefranova O. V. The engineering method of calculation of the remaining life of the bus body safe operation on the basis of estimation of its corrosion deterioration. ARPN

Journal of Engineering and Applied Sciences. - T. 10. № 22. 10511-10522.

[6] Genta G. 2009. Automotive chassis. Volume 1: Components design. G. Genta, L. Morello. - Springer. p. 621.

[7] Genta G. 2009. Automotive chassis. Volume 2: System design. G. Genta, L. Morello. - Springer. p. 825.

[8] Basov K. A. 2005. ANSYS: User's reference book. Moscow: DMK Press. p. 640.

[9] Gepner B., Bojanowski C., Kwasniewski L. and Wekezer J. 2014. Effectiveness of ECE R66 and FMVSS 220 standards in rollover crashworthiness assessment of paratransit buses. International Journal of Automotive Technology. 15(4): 581-591.

[10] Li Z., Xiao Y., Zhu W. and Zhao H. 2013. The safety of body structure and occupant protection research of medium bus under three kinds of frontal impact forms. Volume 197 Lecture Notes in Electrical Engineering. 9: 279-292.

[11] Jeyakumar P. D., Devaradjane G. 2012. Improvement of the frontal structure of a bus for crash accidents. ASME International Mechanical Engineering Congress and Exposition, Proceedings (IMECE). 11: 183-187.

[12] Wang R., Zhang X.-Y., Feng H. and Chen J.-G. 2014. Simulation and improvement of bus rollover against barrier. Zhendong yu Chongji. Journal of Vibration and Shock. 33(6): 40-43.

[13] Bojanowski C., Kwasniewski L., and Wekezer J. W. 2013. Comprehensive Rollover Testing of Paratransit Buses. International Journal of Heavy Vehicle Systems. 20: 76-98.

[14] Rogov Petr Sergeevich, Orlov Lev Nikolaevich. 2015. Verification of Computer Simulation Results of Bus Body Section Rollover. Journal of Traffic and Transportation Engineering. 3(2).

[15] Kalmykov B., Fetisov C., Melnikov A. 2017. The impact of changes in volume of bus body passive safety design. The world of transport and technological machines. 3: 87-93.

[16] Na J., Yuan Z., Gao J. 2015. A Novel Method for Bending Stiffness Evaluation of Bus Body. Advances in Mechanical Engineering. 7(1).

[17] Ovchinnikov N. A. 2019. Modelling and evaluation of the stressed-deformed pillar of a body shell of the bus involving physical non-linearity: AIP Conference Proceedings. XV International Scientific-Technical Conference «Dynamics of Technical Systems», DTS 2019. C. 050036.